

Effect of Bismuth Ions on the Structural, Dielectric and Morphological Properties of Aluminum Doped Yttrium Iron Garnet Nanoparticles Powders Synthesized by Sol-Gel Auto-Combustion Method

RAMESHWAR B. BORADE¹, S.B. KADAM², SAGAR E. SHIRSATH³,
R.H. KADAM⁴, A.B. KADAM^{1,*}

¹Department of Physics, Jawahar Art Science and Commerce College, Andur, Osmanabad, MS, India

²Department of Physics, L.B.S. college, Partur, Jalna, 431501, MS, India

³School of Materials Science and Engineering, U.N.S.W., Kensington, Sydney, NSW 2052, Australia

⁴Department of Physics, Shrikrishna Mahavidyalaya, Gunjoti, Osmanabad 413613, MS, India

*Corresponding author Email: drabkadam@gmail.com

Abstract

The nanocrystalline $Y_{3-x}Bi_xAl_{0.5}Fe_{4.5}O_{12}$ powders with $x = 0.0, 0.5, 1.0, 1.5$ and 2.0 composition were synthesized by a sol-gel auto-combustion route. The elemental compositions of the synthesized samples were confirmed by the EDAX. The structural properties were studied by using X-ray diffractometry (XRD). The morphology of the samples was studied with the help of transmission electron microscopy (TEM). The frequency dependence dielectric measurements were carried out by LCR-Q meter. The micrographs of TEM established that nanoparticles are nano-sized grains with the cluster. The particle sizes are in 100-150 nm range observed from the TEM. It is observed that the porosity and specific surface area decreases with increasing Bi composition. The dielectric permittivity and dielectric loss tangent decreases with applied frequency and follow Maxwell-Wagner's two-layer model. The dielectric parameters were found to be increases with the substitution of bismuth concentration. AC conductivity increases with applied frequency and Bi composition.

Keywords: Stoichiometric; structural; morphological; dielectric properties

INTRODUCTION

Yttrium iron garnet has superior properties like low magnetization, low dielectric loss behavior, low propagation and high electrical resistivity hence it is used in microwave devices [1, 2]. The properties of yttrium iron garnet (YIG) can be altered for the specific application by substituting magnetic and non-magnetic dopants in YIG. Trivalent ion substituted YIG is an important substance used in magneto-optical devices [3, 4]. Yttrium iron garnets crystallize in the cubic crystal structure, exist three crystallographic lattices a, b and c sites. The non-magnetic Y^{3+} ion occupy dodecahedral sites 24(c), magnetic Fe^{3+} ions occupy both octahedral 16(a) and tetrahedral 24(d) sites. The structural, electrical, dielectric, magnetic properties of YIG can be changed by substituting various trivalent ions like Dy^{3+} , Ce^{3+} , Er^{3+} , Tb^{3+} or Bi^{3+} with dodecahedral sited Y^{3+} ion [5, 6]. In the recent years, many researchers work on YIG and substituted YIG. Ftema W. Aldeba et al [7] fabricated $Tb_xY_{3-x}Fe_5O_{12}$ by sol-gel method. They observed nanoparticles prepared with 40-59 nm grain size. Rodziah et al [8] prepared indium substituted YIG and observed that the FMR linewidth broadening decreases up to $x = 0.3$ after that FMR increases. G. B. Turpin [9] explains the anisotropy in the electrical resistivity of Ca-substituted YIG. Hongjie Zhao et al [10] prepared $Bi_xY_{3-x}Fe_5O_{12}$ using the sol-gel route. They reported that the dielectric constant and loss reduces with the substitution of Bi.

However, there is no literature present on the substitution Bi^{3+} in the Al-doped yttrium iron garnet nanoparticle powder. Therefore, we have prepared $\text{Y}_{3-x}\text{Bi}_x\text{Al}_{0.5}\text{Fe}_{4.5}\text{O}_{12}$ ($x = 0.0, 0.5, 1.0, 1.5$ and 2.0) nanoparticle powders using sol-gel route. The powders and pellets were sintered at 1150°C for 10 h. This study is focused on the substitution of Bi^{3+} on Al-doped YIG. In order to gain further knowledge about the effect of bismuth composition on stoichiometric, structural, morphological and dielectric properties were studied and discussed in detail.

EXPERIMENTAL WORK

Bi-substituted aluminum doped YIG ($\text{Y}_{3-x}\text{Bi}_x\text{Al}_{0.5}\text{Fe}_{4.5}\text{O}_{12}$; $x = 0.0, 0.5, 1.0, 1.5, 2.0$) nanocrystalline in the form of the powders and pellets were prepared by the sol-gel auto-combustion route from the nitrates, citric acid and then both were sintered at 1150°C for 10 h. The elemental composition was confirmed by energy dispersive X-ray spectroscopy (EDAX, INCA Oxford, attached to the FE-SEM). The shape, morphology and grain size of the prepared samples were investigated by transmission electron microscopy (TEM, Philips CM-200). LCR-Q meter was used to study dielectric properties with applied frequency (50 Hz - 50 MHz) using silver paste contact.

RESULT AND DISCUSSION

Compositional analysis

Energy dispersive X-ray EDAX analysis was carried out to confirm the chemical composition of selected prepared samples of $\text{Y}_{3-x}\text{Bi}_x\text{Al}_{0.5}\text{Fe}_{4.5}\text{O}_{12}$ ($x = 0.0$ and 2.0) garnet nanoparticles. The EDAX pattern of the selected samples $\text{Y}_{3-x}\text{Bi}_x\text{Al}_{0.5}\text{Fe}_{4.5}\text{O}_{12}$ ($x = 0.0$ and 2.0) are shown Fig 1. From the pattern, the presence of peaks of the elements Y, Bi, Al, Fe, and O is the evidence of formation a pure and Bi-substituted garnet. The compositional percentages observed by EDAX of all the elements are approximately equal to the stoichiometric calculations of synthesized samples. The error of stoichiometric ratios of all the elements present in $\text{Y}_{3-x}\text{Bi}_x\text{Al}_{0.5}\text{Fe}_{4.5}\text{O}_{12}$ ($x = 0.0$ and 2.0) is 1–2%.

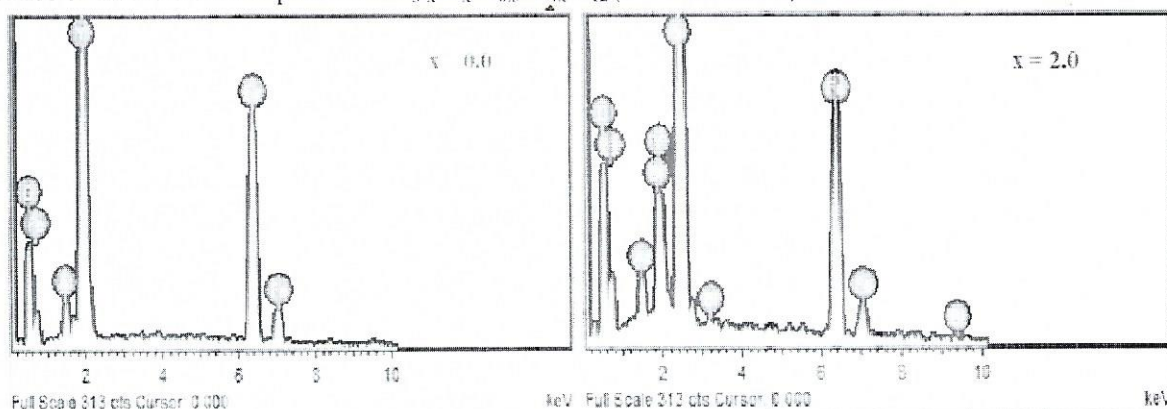


Figure 1. EDAX analysis of $\text{Y}_2\text{Bi}_1\text{Al}_{0.5}\text{Fe}_{4.5}\text{O}_{12}$ ($x = 0.0$ and 2.0) nanoparticles annealed at 1150°C

Structural analysis

The X-ray diffraction patterns of $\text{Y}_{3-x}\text{Bi}_x\text{Al}_{0.5}\text{Fe}_{4.5}\text{O}_{12}$ ($x = 0.0, 0.5, 1.0, 1.5, 2.0$) reported in previous work investigating the phase formation, lattice parameter, grain size and X-ray density. In the present study, we discussed further structural properties. The bulk density was calculated by the eq. 1 [11]

$$d_B = m / \pi r^2 t \quad (1)$$

Where, m , r and t be the mass, radius and thickness of circular plate respectively. The percentage porosity was computed from the eq. 2 [12] $\% P = (1 - d_B/d_x) \times 100$

(2)

Where d_x and d_B are the X-ray and bulk density of the prepared samples respectively.

Table 1 Structural properties of $Y_{3-x}Bi_xAl_{0.5}Fe_{4.5}O_{12}$ ($x = 0.0, 0.5, 1.0, 1.5, 2.0$) nanoparticle

Composition (x)	Bulk density (g/cc)	Porosity (P %)	Specific surface area (m ² /g)
0.0	2.58	98.05	101.60
0.5	3.03	81.74	84.78
1.0	3.34	76.68	84.70
1.5	3.83	65.39	81.80
2.0	4.38	55.58	75.05

The specific surface area (S) was calculated by using the relation $S=6000/Dd_B$ [13] where d_B is the bulk density and D is the average particle size. The obtained values bulk density; porosity and specific surface area are summarized in table 1. It is observed that the bulk density increases with increasing bismuth composition. This is because of the increase in molecular weight which is proportional to the density [14]. The molecular weight of the prepared samples are found to increase from 723.50 g/mol to 963.65 g/mol as the composition of Bi increases from $x = 0.0$ to $x = 2.0$. Hence, bulk density increases with Bi^{3+} ions in the Al-doped YIG. From Fig 2, it is observed that the percentage porosity progressively decreased with the increase of Bi^{3+} ion substitution because the bulk density and porosity was inversely proportional to each other. The specific surface area (shown in Table 1) decreased with increasing Bi content in YIG. This decrease of S is due to the increase in particle size and density.

Morphological analysis

The transmission electron microscopy technique was used to observe the surface morphology clearly and confirm the phase structure of the prepared sample. Fig. 3 shows the TEM micrographs and corresponding electron diffraction patterns of the $Y_{3-x}Bi_xAl_{0.5}Fe_{4.5}O_{12}$ ($x = 0.0$ and $x = 2.0$) nanocrystalline powder sintered at 1150 °C. Due to the overlapping of the particles, it is difficult to determine the nanoparticle size. However, the average particle size from TEM photograph is around 100-150 nm. Fig. 3 (a and b) shows that the nanoparticles are in elliptical or star-like shape. This is because of the formation of agglomeration of nanoparticles. The formation of agglomeration is due to the interaction between magnetic nanoparticles. The selected area electronic diffraction (SAED) pattern of the nanoparticles is shown in Fig. 3 (c and d). The selected electron diffraction patterns show the spotty rings indicating the polycrystalline of the samples. The indexed diffraction rings confirm the crystal planes of yttrium iron garnet. The interplanar distance is 0.27 nm, which is corresponding to the d value of the diffraction peak (420). Therefore, the nanocrystalline powder was successfully prepared by the sol-gel route.



Principal

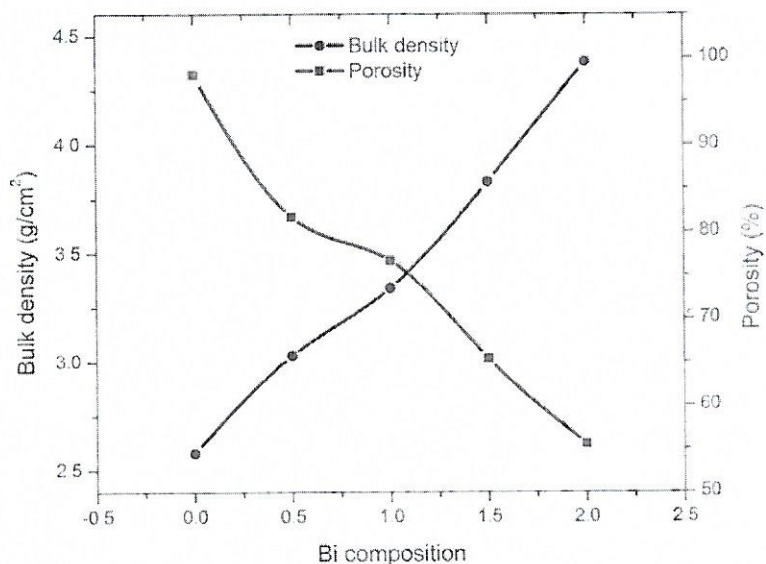


Figure 2. Variation bulk density and percentage porosity as function of Bi concentration in samples

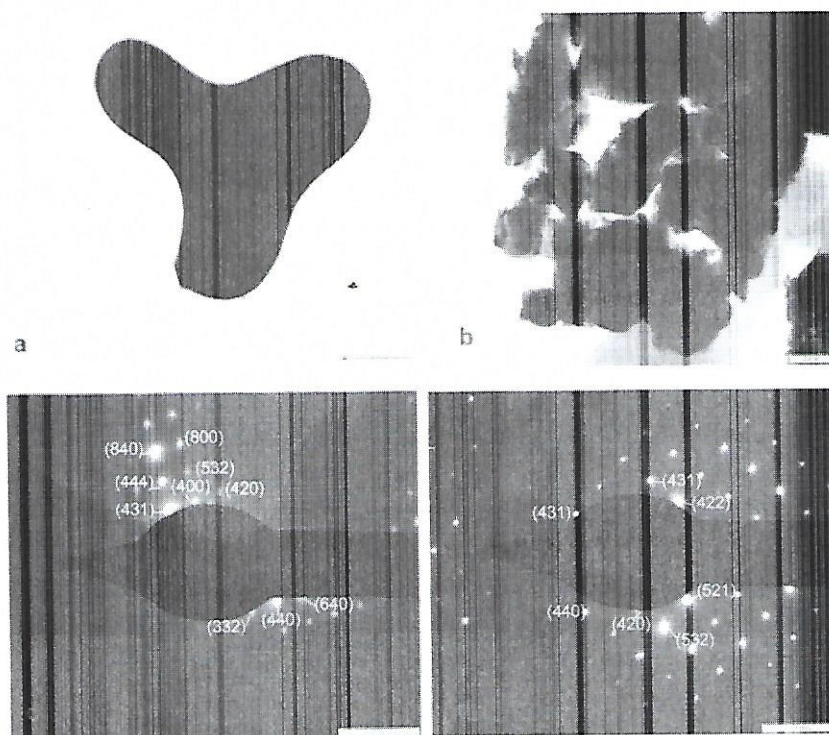


Figure 3. The TEM images of (a) $x = 0.0$, (b) $x = 2.0$ and SAED pattern of (c) $x = 0.0$, (d) $x = 2.0$ of $Y_{3-x}Bi_xAl_{0.5}Fe_{4.5}O_{12}$ samples

Frequency dependence of dielectric properties

Fig.4 (a and b) shows the frequency dependent real and imaginary parts of complex dielectric constant with applied frequency (50Hz-5 MHz) of $Y_{3-x}Bi_xAl_{0.5}Fe_{4.5}O_{12}$ ($x = 0.0, 0.5, 1.0, 1.5$ and 2.0) at room temperature. It has been seen that the real and imaginary parts of dielectric constant decreases continuously with increase in frequency, showing dielectric behavior as published in the literature. The decrease in the dielectric constant is at lower frequencies and became constant at higher frequencies. It was found that the polarization decreases with increase in frequency and gets a stable value at a particular higher frequency. This can be explained that beyond certain applied frequency the electron exchange among the ferrous ion and ferric ion does not follow the AC field. Maxwell-Wagner's two-layer model in agreement with Koop's phenomenological theory explained this dispersion mechanism at low frequency. It was found that the dielectric constant increases with increasing Bi composition. This is might be due to the extra hopping process between Bi^{3+} and Bi^{2+} ions. The Bi substitution changes polarization mechanism of garnet by the ions relaxation polarization and electrons-holes relaxation polarization. Therefore dielectric behavior depends on the local displacement of electrons and ions in the applied AC field.

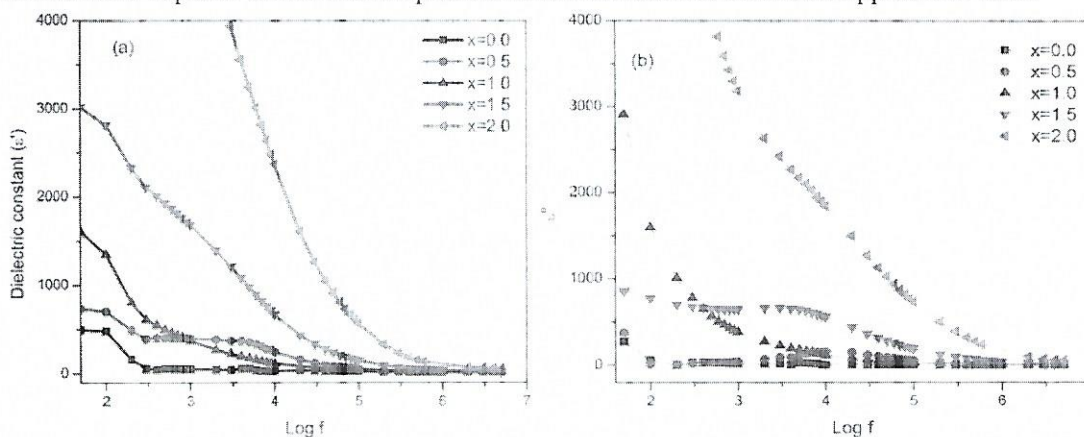


Figure 4. Variation of (a) real and (b) imaginary part of dielectric constant with frequency for $Y_{3-x}Bi_xAl_{0.5}Fe_{4.5}O_{12}$ ($x = 0.0, 0.5, 1.0, 1.5, 2.0$)

The variation of dielectric loss tangent ($\tan \delta$) as a function of frequency ($\log f$) at room temperature for all the samples of $Y_{3-x}Bi_xAl_{0.5}Fe_{4.5}O_{12}$ is shown in Fig. 5. It is observed that the dielectric loss decreases as the frequency of the applied external field increases. A resonance peak is observed in the dielectric loss tangent versus frequency. These resonance peaks are appearing due to resonance behavior, when the natural frequency of jumping ions becomes equal to the frequency of the external applied alternating electric field. It has been observed that height of peak increases and the peak shifts towards higher frequency with increasing Bi composition in YIG. At resonance, the maximum electrical energy is going to the vibrating ions and a peak is observed as a effect of power loss. Since the number of holes increases with increasing Bismuth composition, which results in an increase of the mobility of charge carriers, therefore, the peak shifts towards the higher frequency. The condition $\omega\tau = 1$ ($\omega = 2\pi f_{max}$) is satisfying for observing maxima in dielectric loss tangent of a material. The values of dielectric loss tangent increases from 0.21 to 0.98 as Bismuth concentration increases from $x = 0.0$ to $x = 2.0$.

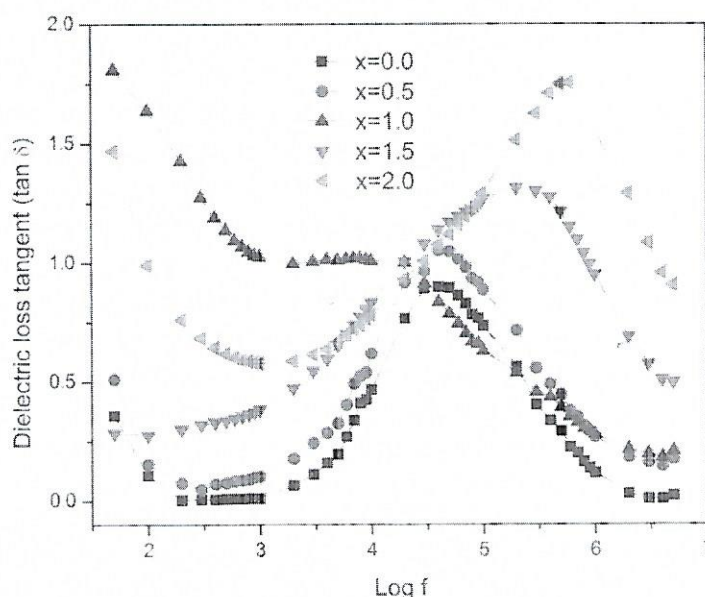


Figure 5. Variation of dielectric loss with log frequency for $Y_{3-x}Bi_xAl_{0.5}Fe_{4.5}O_{12}$ ($x = 0.0 - 2.0$)

In order to understand the conduction mechanism, the AC conductivity can be evaluated from the dielectric data using the relation [15], $\sigma_{AC} = \omega \epsilon_0 \epsilon''$ (3)

Where, ϵ'' is imaginary parts of complex dielectric permittivity ϵ_0 is permittivity of free space and ω is the angular frequency.

Table 2. AC conductivity and dielectric loss tangent for $Y_{3-x}Bi_xAl_{0.5}Fe_{4.5}O_{12}$ ($x = 0.0 - 2.0$) nanoparticles

Composition (x)	AC conductivity (S/cm)	Dielectric loss tangent
0.0	1.19×10^{-7}	0.21
0.5	9.34×10^{-7}	0.43
1.0	1.99×10^{-6}	0.79
1.5	9.66×10^{-6}	0.78
2.0	3.11×10^{-5}	0.98

The variation of AC conductivity with applied frequency at room temperature as a function of Bi^{3+} ion substitution in YIG is illustrated in Fig. 6. From the plots it is found that AC conductivity increases with the frequency of applied field linearly, this is because of the increase in frequency increase the hopping frequency of the charge carriers. Thus, AC conductivity is proportional to angular frequency resulted the linear nature. The conductivity in garnets is due to the transportation of electrons via Fe^{2+}/Fe^{3+} ions or Bi^{2+}/Bi^{3+} ions at neighboring layers. The increase in AC conductivity at higher frequencies might be due to a reduction in the space charge polarization at higher frequencies. Thus AC electrical conductivity increases with increases in frequency [16, 17]. The conductivity of the samples increases with increase in Bi^{3+} concentration as shown in Table 2.

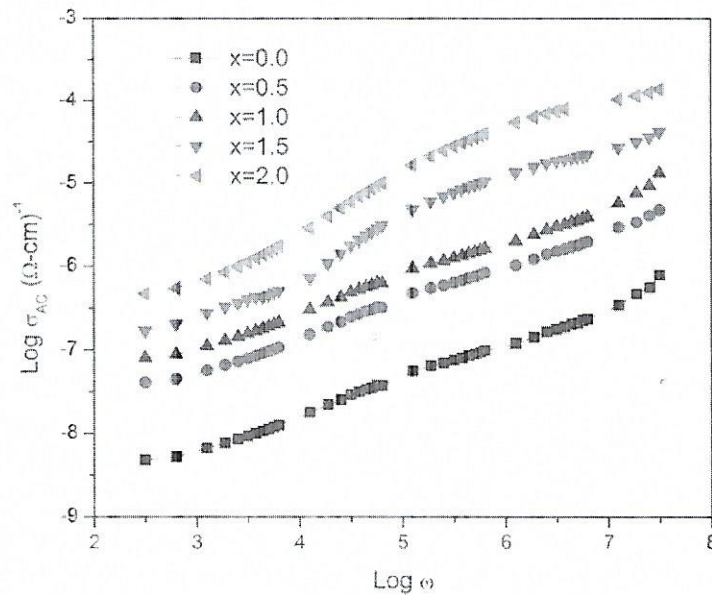


Figure 6. The variation of AC conductivity with applied frequency as a function of Bi³⁺ ion substitution in YIG

CONCLUSIONS

In present the study, The EDAX pattern shows that nanoparticles prepared in good stoichiometric ratios and no other element interfere in the sample. The porosity and specific surface area were found to be decreases with increasing Bi composition due to the increase of bulk density. TEM study revealed that Bi-substituted YAIG composed in nanocrystals form with some agglomeration. The dielectric constant, dielectric loss tangent ($\tan \delta$) and AC conductivity (σ_{AC}) increases with Bismuth content. The dielectric permittivity and dielectric loss tangent decreases with applied frequency. These behaviors of frequency dependent dielectric parameters were explained on the basis of electron-hole hopping mechanism. In this study, the samples show excellent properties such as homogenous structure, small grain size, and dielectric which have potential uses in microwave devices.

REFERENCES

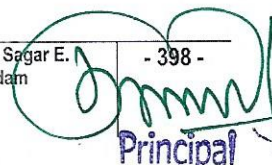
- [1] V.G. Harris, A. Geiler, Y. Chen, S.D. Yoon, M. Wu, A. Yang, Z. Chen, P. He, P.V. Parimi, X. Zuo, Recent advances in processing and applications of microwave ferrites, *Journal of Magnetism and Magnetic Materials*, 321 (2009) 2035-2047.
- [2] J.D. Adam, L.E. Davis, G.F. Dionne, E.F. Schloemann, S.N. Stitzer, Ferrite devices and materials, *IEEE Transactions on Microwave Theory and Techniques*, 50 (2002) 721-737.
- [3] E. Garskaite, K. Gibson, A. Leleckaite, J. Glaser, D. Niznansky, A. Kareiva, H.-J. Meyer, On the synthesis and characterization of iron-containing garnets (Y₃Fe₅O₁₂, YIG and Fe₃Al₅O₁₂, IAG), *Chemical physics*, 323 (2006) 204-210.
- [4] S. Higuchi, S. Takekawa, K. Kitamura, Magneto-optical properties of cerium-substituted yttrium iron garnet single crystals grown by traveling solvent floating zone method, *Japanese journal of applied physics*, 38 (1999) 4122.
- [5] Z. Cheng, H. Yang, Y. Cui, L. Yu, X. Zhao, S. Feng, Synthesis and magnetic properties of Y_{3-x}Dy_xFe₅O₁₂ nanoparticles, *Journal of magnetism and magnetic materials*, 308 (2007) 5-9.


Principal

03



- [6] R. Shaiboub, N.B.y. Ibrahim, M. Abdullah, F. Abdulhade, The physical properties of erbium-doped yttrium iron garnet films prepared by sol-gel method, *Journal of Nanomaterials*, 2012 (2012) 2.
- [7] F.W. Aldbea, N. Ibrahim, M.H. Abdullah, R.E. Shaiboub, Structural and magnetic properties of $Tb_xY_{3-x}Fe_5O_{12}$ ($0 \leq x \leq 0.8$) thin film prepared via sol-gel method, *Journal of sol-gel science and technology*, 62 (2012) 483-489.
- [8] R. Nazlan, M. Hashim, I. Ismail, J. Hassan, Z. Abbas, F.M. Idris, I.R. Ibrahim, Compositional and frequency dependent-magnetic and microwave characteristics of indium substituted yttrium iron garnet, *Journal of Materials Science: Materials in Electronics*, 28 (2017) 3029-3041.
- [9] G. Turpin, R. Bornfreund, P. Wigen, A. Lehmann-Szweykowska, Anisotropy in the electrical resistivity of Ca-substituted yttrium iron garnet thin films, *Journal of applied physics*, 81 (1997) 4872-4874.
- [10] H. Zhao, J. Zhou, Y. Bai, Z. Gui, L. Li, Effect of Bi-substitution on the dielectric properties of polycrystalline yttrium iron garnet, *Journal of magnetism and magnetic materials*, 280 (2004) 208-213.
- [11] R. Kadam, A. Birajdar, S.T. Alone, S.E. Shirsath, Fabrication of $Co_{0.5}Ni_{0.5}Cr_xFe_{2-x}O_4$ materials via sol-gel method and their characterizations, *Journal of Magnetism and Magnetic Materials*, 327 (2013) 167-171.
- [12] S.E. Shirsath, B. Toksha, R. Kadam, S. Patange, D. Mane, G.S. Jangam, A. Ghasemi, Doping effect of Mn^{2+} on the magnetic behavior in Ni-Zn ferrite nanoparticles prepared by sol-gel auto-combustion, *Journal of Physics and Chemistry of Solids*, 71 (2010) 1669-1675.
- [13] C.J. Brinker, G.W. Scherer, *Sol-gel science: the physics and chemistry of sol-gel processing*, Academic press, 2013.
- [14] V. Chaudhari, S.E. Shirsath, M. Mane, R. Kadam, S. Shelke, D. Mane, Crystallographic, magnetic and electrical properties of $Ni_{0.5}Cu_{0.25}Zn_{0.25}La_xFe_{2-x}O_4$ nanoparticles fabricated by sol-gel method, *Journal of Alloys and Compounds*, 549 (2013) 213-220.
- [15] P. Jadhav, M. Shelar, B. Chougule, Synthesis and Property Measurement of Three-Phase ME Composites, *J. Appl. Phys. Res*, 1 (2010) 92-99.
- [16] G.R. Mohan, D. Ravinder, A.R. Reddy, B. Boyanov, Dielectric properties of polycrystalline mixed nickel-zinc ferrites, *Materials Letters*, 40 (1999) 39-45.
- [17] S. Suryavanshi, R. Patil, S. Patil, S. Sawant, DC conductivity and dielectric behavior of Ti^{4+} substituted Mg-Zn ferrites, *Journal of the Less Common Metals*, 168 (1991) 169-174.


Principal